CRYSTAL STRUCTURES AND ANALYSIS OF 1,2,4 TRIAZOLE AND PYRAZOLE COMPOUNDS

by

GOH JIA HAO

UNIVERSITI SAINS MALAYSIA
2011

CRYSTAL STRUCTURES AND ANALYSIS OF 1,2,4 TRIAZOLE AND PYRAZOLE COMPOUNDS

by

GOH JIA HAO

Thesis submitted in fulfillment of the requirements for the Degree of Master of Science

June 2011

ACKNOWLEDGEMENTS

First of all, I owe my deepest gratitude to my family members who have given me the opportunity for postgraduate education. This thesis would not have been possible without their patience, understanding and spiritual support in realizing my dreams.

I am heartily thankful to my supervisor, Professor Fun Hoong Kun, whose supervisions, encouragements and supports from the preliminary to the final stage enabled me to complete my thesis successfully. His continual and convincing spirit of "Crystallography is Fun and Fun is Crystallography" in concern to research as well as teaching had enabled me to develop a thorough understanding of X-ray Crystallography. Besides that, I would like to dedicate my heartfelt gratitude also to my co-supervisor, Associate Professor Abdul Razak Ibrahim for his untiring effort, commitment and guidance throughout my studies.

In addition, I greatly thank Universiti Sains Malaysia and Institute of Postgraduate Studies, USM for a wide range of facilities and supports provided as well as the USM Fellowship awarded. Financial support provided by the Research University Golden Goose Grant (1001/PFIZIK/811012) and the Science Fund (305/PFIZIK/613312) are also acknowledged. Besides that, it is my pleasure to thank fellow researchers from India especially Professor B. Kalluraya and Associate Professor Arun M. Isloor, for providing research samples and cooperation in journal publications.

Last but not least, I am greatly appreciative of all members of X-ray Crystallography Unit, School of Physics, Universiti Sains Malaysia for their kind and helpful cooperation throughout my research in the laboratory.

TABLE OF CONTENTS

CHAPTER 3 – MATERIALS AND METHODS

LIST OF TABLES

LIST OF FIGURES

LIST OF PLATES

STRUKTUR-STRUKTUR HABLUR DAN ANALISIS-ANALISIS SEBATIAN 1,2,4-TRIAZOL DAN PIRAZOL

ABSTRAK

Penyelidikan ini adalah bertujuan untuk mengkaji struktur-struktur hablur bagi sebatian-sebatian 1,2,4-triazol dan pirazol yang berperanan penting dalam aspek biologi dan farmakologi dengan kaedah kristalografi sinar-X hablur tunggal. Satu siri yang terdiri daripada sembilan sebatian bagi terbitan 1,2,4-triazol dan satu siri yang terdiri daripada enam sebatian bagi terbitan pyrazol disintesis dan dihablur untuk mendapatkan hablur tunggal. Data dikumpul dengan menggunakan diffraktometer-diffraktometer CCD Bruker SMART APEXII atau Bruker APEXII DUO. Struktur diselesaikan dengan kaedah terus dan disempurnakan dengan kaedah kuasa-dua terkecil. Parameter-parameter geometri dan penyusunan hablur diperoleh dan akhirnya perbandingan mudah telah dilakukan untuk beberapa struktur yang berkaitan. Keputusan kajian menunjukkan lapan daripada sebatian tersebut telah menghablur dalam kumpulan ruang monoklinik $P2_1/c$, lima dalam kumpulan ruang triklinik $P\bar{1}$ manakala dua lagi dalam kumpulan ruang monoklinik $C2/c$. Parameter-parameter geometri yang diperhati adalah dalam julat normal dan adalah konsisten dengan yang diperhati dalam struktur-struktur yang berkaitan. Tiada ikatan hidrogen antara molekul diperhati untuk dua sebatian manakala sebatian-sebatian yang lain membentuk ikatan hidrogen antara molekul dalam struktur hablur. Interaksi lemah antara molekul juga dapat diperhati dalam beberapa sebatian tersebut. Sebagai perbandingan, walaupun beberapa struktur yang berkaitan dihablur dalam kumpulan

ruang yang berbeza, struktur-struktur hablur tersebut adalah berpadanan dan mempunyai persamaan dalam geometri molecular.

CRYSTAL STRUCTURES AND ANALYSIS OF 1,2,4-TRIAZOLE AND PYRAZOLE COMPOUNDS

ABSTRACT

The purpose of this research is to study the crystal structures of some biologically and pharmacologically important 1,2,4-triazole and pyrazole compounds by single crystal X-ray crystallography method. A series of nine compounds of 1,2,4-triazole derivatives and a series of six compounds of pyrazole derivatives were synthesized and crystallized to obtain single crystals. The data was collected using either Bruker SMART APEXII or Bruker APEXII DUO CCD area-detector diffractometers. The structures were solved by direct methods and refined by least-squares method. The geometrical parameters as well as crystal packing were obtained and finally simple comparisons were undertaken for some closely related structures. Results showed that eight of the compounds crystallized in the monoclinic space group $P2_1/c$, five in the triclinic space group $P\bar{1}$ and the remaining two in the monoclinic space group $C2/c$. The geometrical parameters observed are within normal ranges and consistent to those observed in related structures. No intermolecular hydrogen bond is observed for two compounds whereas the remaining compounds form hydrogen-bonded crystal structures. Weak intermolecular interactions are also observed in some of these compounds. For comparison, although some closely related structures crystallized in different space groups, they are having closely similar molecular geometries and fit fairly well with each other.

CHAPTER 1 – INTRODUCTION

In this thesis, a series of nine compounds of 1,2,4-triazole derivatives (**Compounds 1**, **2**, **3**, **4**, **5**, **6**, **7**, **8** and **9**) and a series of six compounds of pyrazole derivatives (**Compounds 10**, **11**, **12**, **13**, **14** and **15**) were determined and analyzed by single crystal X-ray analysis method. The crystal samples were synthesized and crystallized by fellow researchers from Department of Studies in Chemistry, Mangalore University, Mangalagangotri, Mangalore, India and Department of Chemistry, National Institute of Technology-Karnataka, Surathkal, Mangalore, India.

All the crystal data were collected using either Bruker SMART APEXII or Bruker APEXII DUO CCD area-detector diffractometers (Bruker, 2009) at X-ray Crystallography Unit, School of Physics, Universiti Sains Malaysia (USM), Penang, Malaysia. The experimental results obtained were analyzed and have been published in *Acta Crystallographica Section E: Structure Reports Online*.

In this chapter, brief introductions of X-ray crystallography, general backgrounds and applications of 1,2,4-triazole and pyrazole derivatives as well as the research objective are presented. Basic principles of X-rays structure analysis are discussed in details in the next chapter.

1.1 X-ray Crystallography

X-ray crystallography is an analytical technique in which X-ray diffraction methods are employed to determine the actual three-dimensional arrangement of atoms in a crystalline structure. The science of X-ray crystallography originated with the discovery by Max von Laue in 1912 that crystals diffract X-ray radiations. Since then, single crystal

X-ray crystallography has developed into the most powerful method for obtaining the atomic arrangement in crystalline state.

Structure analysis by X-ray crystallography can be applied to a wide range of structure sizes, from small organic molecules and simple salts, to complex minerals, synthetically prepared inorganic and organo-metallic complexes, natural product compounds as well as to biological macromolecules, such as proteins and viruses.

The precise information of molecular geometry is important in nearly all fields of chemical and biological researches. The three-dimensional atomic coordinates can be easily obtained from the comprehensive crystallographic databases such as the Cambridge Structural Database (CSD) and Protein Data Bank. Crystallographic analyses are always the starting point for molecular modeling as well as drug design. In fact, many of most significant advances in structural chemistry and structural biology are based upon X-ray crystallography analyses.

Generally, the results obtained from X-ray crystallography analyses are complementary to other commonly used solid-state techniques such as X-ray powder diffraction, solid-state NMR, EPR, FT-IR and Raman spectroscopy, and neutron diffraction. Chemists also routinely use such techniques as nuclear magnetic resonance, infrared and ultraviolet spectroscopy, mass spectrometry, x-ray fluorescence, and elemental analysis for the identification and characterization of compounds prepared. After suitable analysis and interpretation, the experimental results obtained from these techniques may yield important information concerning the composition and structure of the compound. However, such information is always incomplete, fragmentary and ambiguous. There are a number of classes of chemical compounds such as natural product compounds, organo-metallic complexes, inorganic salts, metal cluster systems, organic and inorganic reaction products for which the complete structure cannot be deduced even with all of the other methods combined. X-ray crystallography is uniquely capable of unambiguously determining the complete three-dimensional molecular structures (including the absolute stereochemistry) of chemical substances.

1.2 1,2,4-Triazole Derivatives

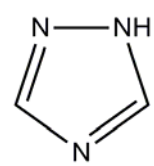

Figure 1.1 Schematic diagram of 1,2,4-triazole

1,2,4-Triazole [systematic name: 1*H*-1,2,4-triazole], with molecular formula $C_2H_3N_3$, is one of a class of simple organic heterocyclic compounds containing a five-membered ring composed of three nitrogen atoms and two carbon atoms at non-adjacent positions. A degree of respectability has been bestowed upon 1,2,4-triazole derivatives due to their various pharmacological activities such as analgesic (Amir & Shikha, 2004), anti-helminthic (Holla *et al.*, 2003), anti-oxidant (Kuş *et al.*, 2008), anti-tuberculosis (Walczak *et al.*, 2004), anti-cancer (Bekircan & Bektas, 2006; Sztanke *et al.*, 2008), anti-convulsant (Almasirad *et al.*, 2004; Bekircan & Bektas, 2006), anti-fungal (Amir *et al.*, 2008; Bekircan & Bektas, 2006; Holla *et al.*, 2003), anti-bacterial (Amir *et al.*, 2008; Bekircan & Bektas, 2006; Holla *et al.*, 2003), anti-microbial (Demirbas *et al.*, 2004; Sztanke *et al.*, 2008; Turan-Zitouni *et al.*, 2005), anti-tumor (Al-Soud *et al.*, 2003; Amir *et al.*, 2008; Demirbas *et al.*, 2004) and anti-inflammatory (Amir & Shikha, 2004; Amir *et al.*, 2008; Bekircan & Bektas, 2006; Sujith *et al.*, 2009). They also act as effective pesticides (Koparır *et al.*, 2005). Some of the present day drugs such as Ribavirin (anti-viral agent), Rizatriptan (anti-migraine agent), Alprazolam (anxiolytic agent), Fluconazole and Itraconazole (anti-fungal agents) are the best examples of potent molecules possessing the triazole nucleus (Fun *et al.*, 2009). Furthermore, the amino and mercapto groups of thio-substituted 1,2,4-triazole serve as readily accessible nucleophilic centers for the preparation of N-bridged heterocycles.

1.2.1 Preparation of 1,2,4-Triazole Derivatives

1,2,4-Triazole derivatives can be prepared using the Einhorn-Brunner reaction or Pellizzari reaction (1,2,4-Triazole, 2011).

Einhorn-Brunner Reaction:

The chemical reaction of imides with alkyl hydrazines to form a mixture of isomeric 1,2,4-triazole (Einhorn-Brunner reaction, 2011).

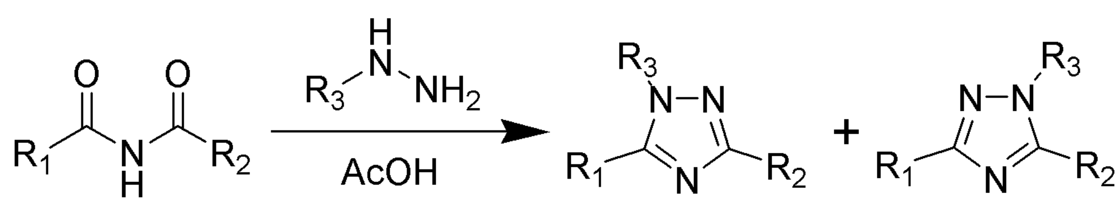

Figure 1.2 Einhorn-Brunner reaction scheme

Pellizzari Reaction:

The chemical reaction of amide with hydrazide to form a 1,2,4-triazole (Pellizzari reaction, 2011).

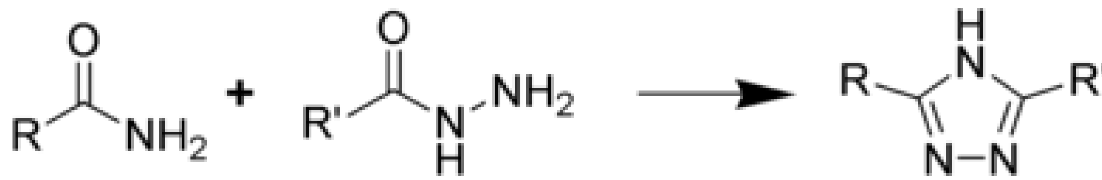

Figure 1.3 Pellizzari reaction scheme

1.2.2 Applications of 1,2,4-Triazole Derivatives

1,2,4-Triazole derivatives find use in a wide variety of applications, most notably as antifungals, such as fluconazole and itraconazole, which are used to treat fungal infections.

Fluconazole

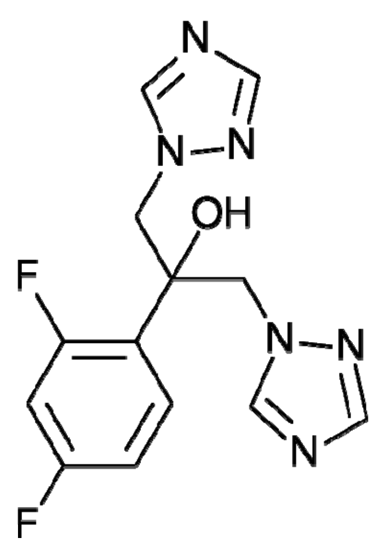

Figure 1.4 Schematic structure of fluconazole, containing two 1,2,4-triazole moieties

Fluconazole is used in the treatment and prevention of superficial and systemic fungal infections. It is commonly marketed under the trade name of **Diflucan®** or **Trican®** (Fluconazole, 2011).

Itraconazole

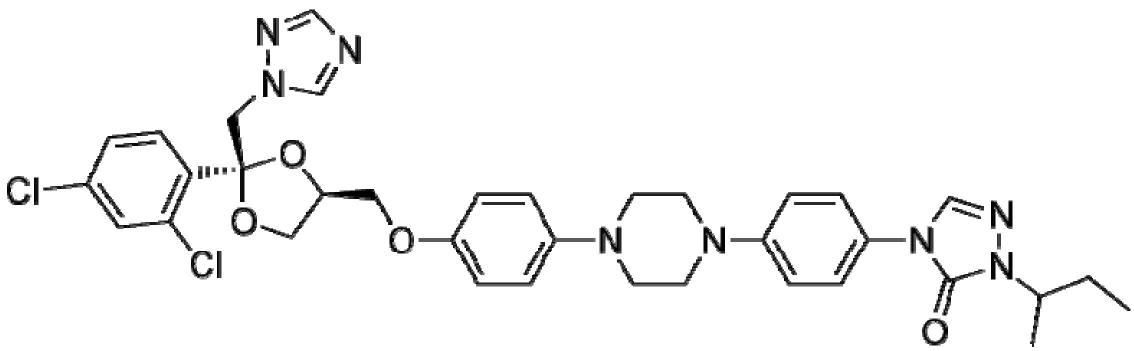

Figure 1.5 Schematic structure of itraconazole, containing two 1,2,4-triazole moieties

Itraconazole is a triazole anti-fungal agent that is prescribed to patients with fungal infections. It is invented in 1984, marketed as **Sporanox®** by Janssen Pharmaceutica (Itraconazole, 2011).

1.3 Pyrazole Derivatives

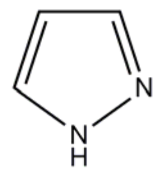

Figure 1.6 Schematic diagram of pyrazole

Pyrazole [systematic name: 1*H*-pyrazole], with molecular formula $C_3H_4N_2$, is one of a class of simple organic heterocyclic compounds containing a five-membered ring composed of three carbon atoms and two nitrogen atoms in adjacent positions. Pyrazole derivatives are in general well-known nitrogen-containing heterocyclic compounds and various procedures have been developed for their synthesis. The 1,3-dipolar cycloaddition reaction with various dipolarphiles offers a convenient synthetic route for the preparation of pyrazole derivatives and been studied extensively (Rai *et al.*, 2008). The chemistry of pyrazole derivatives has been the subject of much interest due to their importance for various applications, and their widespread potential and proven biological and pharmacological activities such as analgesic (Tawab *et al.*, 1960), herbicidal (Rai *et al.*, 2008), tranquilizing (Rai *et al.*, 2008), anti-tumor (Rai *et al.*, 2008), anti-pyretic (Rai *et al.*, 2008, Tawab *et al.*, 1960), anti-inflammatory (Rathish *et al.*, 2009), anti-cancer (Sridhar & Perumal, 2003), anti-malarial (Sridhar & Perumal, 2003) and anti-hyperglycemic (Sridhar & Perumal, 2003) activities. Some alkyl- and aryl-substituted pyrazoles have a sharply pronounced sedative action on the central nervous system (Sridhar & Perumal, 2003). Certain alkyl pyrazoles also show significant bacteriostatic, bacteriocidal, fungicidal, analgesic and anti-pyretic activities (Sridhar & Perumal, 2003).

1.3.1 Preparation of Pyrazole Derivatives

Pyrazoles are produced synthetically through the reaction of *α,β*-unsaturated aldehydes with hydrazine and subsequent dehydrogenation (Pyrazole, 2011).

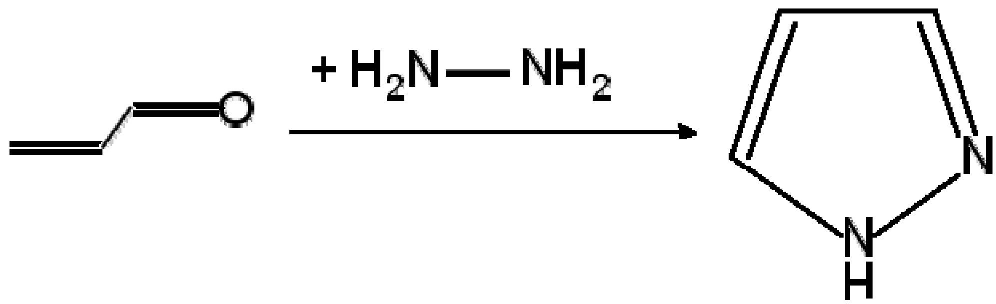

Figure 1.7 Pyrazole derivatives reaction scheme

1.3.2 Applications of Pyrazole Derivatives

Pyrazole derivatives are widely used as analgesic, anti-inflammatory, anti-pyretic, tranquilizing, anti-diabetic and anti-bacterial activities. Celecoxib and Metamizole sodium are two of the famous applications of pyrazole derivatives.

Celecoxib

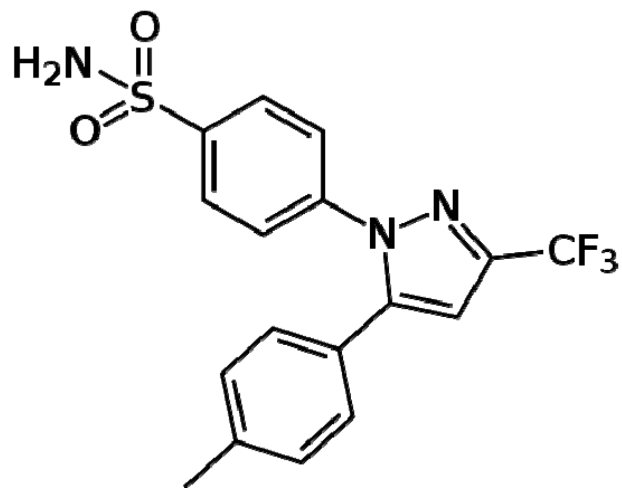

Figure 1.8 Schematic structure of Celecoxib, containing a pyrazole moiety

Celecoxib is a sulfa non-steroidal anti-inflammatory drug (NSAID) used in the treatment of osteoarthritis, rheumatoid arthritis, acute pain and menstrual pain. It is marketed by Pfizer, under the brand name of **Celebrex**® or **Celebra®** (Celecoxib, 2011).

Metamizole sodium

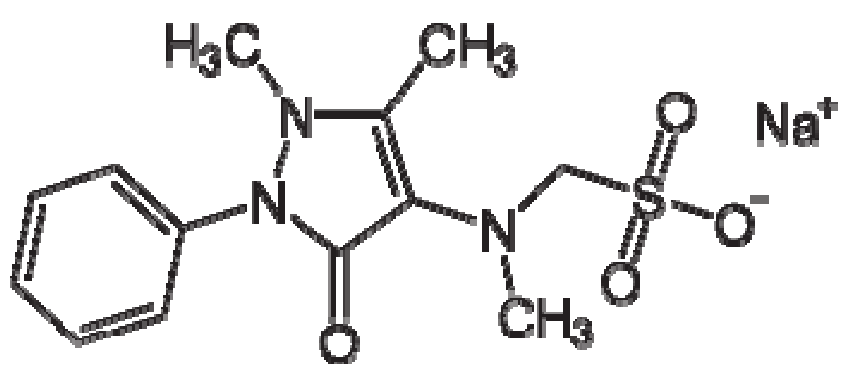

Figure 1.9 Schematic structure of Metamizole sodium, containing a pyrazole moiety

Metamizole sodium or dipyrone is a powerful analgesic and anti-pyretic drug. From a randomized, multinational study involving 555 children showed that metamizole sodium produced a significant greater body temperature reduction than ibuprofen and paracetamol, and it helped to maintain low body temperature for a longer duration. It is marketed in 1920, under various trade names including **Algozone®**, **Algocalmin®**, **Analgin®** and **Dipirona®**. It remained available worldwide until the 1970s, when it was discovered that the drug carries a small risk of causing agranulocytosis, which is lowering white blood cell amount. Several national medical authorities have banned it either totally or have restricted it to be available only on prescription (Metamizole, 2011).

1.4 Research Objective

Due to the proven biological and pharmacological importance of 1,2,4-triazole and pyrazole heterocyclic compounds, the main research objective is to determine and analyze the crystal structures of some unreported 1,2,4-triazole and pyrazole compounds. By using the single crystal X-ray structure analysis, complete set of crystal data of these previously unreported structures can be obtained. All geometric parameters in the molecular structure such as fractional atomic coordinates, bond lengths and angles as well as the three-dimensional crystal packing can also be elucidated.

(a) The X-ray structure analysis of **Compound 1** {4-amino-3-(*p*-tolyloxymethyl)-1*H*-1,2,4-triazole-5(4*H*)-thione} was undertaken to study the biological importance of the 1,2,4-triazole derivatives.

(b) The X-ray structure analysis of **Compound 2** {(*E*)-3-methyl-4-[(2-oxidoquinolin-1-ium-3-yl)methyleneamino]-1*H*-1,2,4-triazole-5(4*H*)-thione *N*,*N*-dimethyl-formamide solvate}, **Compound 3** {(*E*)-4-(4-hydroxy-3-methoxybenzylidene-

amino)-3-[1-(4-isobutylphenyl)ethyl]-1*H*-1,2,4-triazole-5(4*H*)-thione},
Compound 4 {(*E*)-4-[4-fluorobenzylidene]amino}-3-[1-(4-isobutylphenyl)ethyl]-1-(morpholinomethyl)-1*H*-1,2,4-triazole-5(4*H*)-thione methanol hemisolvate} and **Compound 5** {(*E*)-1-[(diphenylamino)methyl]-4-(4-fluorobenzylideneamino)-3-[1-(4-isobutylphenyl)ethyl]-1*H*-1,2,4-triazole-5(4*H*)-thione} were undertaken as part of ongoing research on Schiff base derivatives of 1,2,4-triazole and Mannich bases.

(c) The X-ray structure analysis of **Compound 6** {4-[3-(phenoxymethyl)-7*H*-1,2,4-triazolo[3,4-*b*][1,3,4]thiadiazin-6-yl]-3-(*p*-tolyl)sydnone}, **Compound 7** {3-phenyl-4-{3-[(*p*-tolyloxy)methyl]-7*H*-1,2,4-triazolo[3,4-*b*][1,3,4]thiadiazin-6-yl]-sydnone}, **Compound 8** {4-{3-[(2-isopropyl-5-methylphenoxy)methyl]-7*H*-1,2,4-triazolo[3,4-*b*][1,3,4]thiadiazin-6-yl]-3-(*p*-tolyl)sydnone}, **Compound 9** {4-[3-(1-naphthyloxymethyl)-7*H*-1,2,4-triazolo[3,4,*b*][1,3,4]thiadiazin-6-yl]-3-*p*-tolylsydnone} and **Compound 10** {3-(2,3-dimethyl-5-oxo-1-phenyl-2,5-dihydro-1*H*-pyrazole-4-yl)sydnone} were undertaken as part of ongoing research on 1,2,4-triazole and pyrazole derivatives of sydnone nucleus.

(d) The X-ray structure analysis of **Compound 11** {5-bromo-2-[5-(4-nitrophenyl)-3-phenyl-4,5-dihydro-1*H*-pyrazol-1-yl]pyrimidine} was undertaken to study the biological importance of the pyrazole derivatives.

(e) The X-ray structure analysis of **Compound 12** {[3-(5-nitro-2-furyl)-1-phenyl-1*H*-pyrazol-4-yl](phenyl)methanone}, **Compound 13** {(4-methylphenyl)[3-(5-nitro-2-furyl)-1-phenyl-1*H*-pyrazol-4-yl]methanone}, **Compound 14** {(4-methyl-phenyl)[1-(4-methylphenyl)-3-(5-nitro-2-furyl)-1*H*-pyrazol-4-yl]methanone} and **Compound 15** {(4-chlorophenyl)[1-(4-methylphenyl)-3-(5-nitro-2-furyl)-1*H*-

pyrazol-4-yl]methanone} were undertaken as part of ongoing studies on synthetic route of pyrazole derivatives by 1,3-dipolar cycloaddition carrying nitrofuran moiety.

CHAPTER 2 – BASIC PRINCIPLES OF X-RAY STRUCTURE ANALYSIS

2.1 Generation of X-rays

X-rays, first discovered by Wilhelm Conrad Roentgen in 1892, are electromagnetic radiations with wavelength, λ in the range of $0.1 < \lambda < 100$ Å. Continuous X-rays are produced when high speed electrons hit a target material and are rapidly decelerated. The minimum wavelength of these continuous X-rays obtained is given by

$$E = eV = \frac{hc}{\lambda} \tag{2.1}$$

$$\lambda_{\min} = \frac{hc}{eV} \tag{2.2}$$

where h = Planck's constant $= 6.626 \times 10^{-34} J \cdot s$

c = speed of light = $2.998 \times 10^{8} ms^{-1}$

e = electron charge = $1.602 \times 10^{-19} C$

V = accelerating voltage

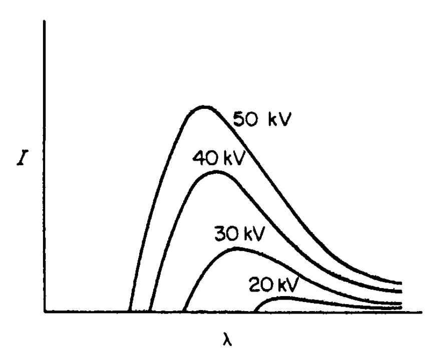

Figure 2.1 Continuous X-ray spectra as a function of accelerating voltage (Stout & Jensen, 1968)

The maximum intensity of the X-ray spectra occurs at longer wavelength. As the accelerating voltage is increased, not only peak intensity and minimum wavelength are moved to shorter, more penetrating wavelengths, but also the total intensity is increased even though the electron current remains the same (Figure 2.1).

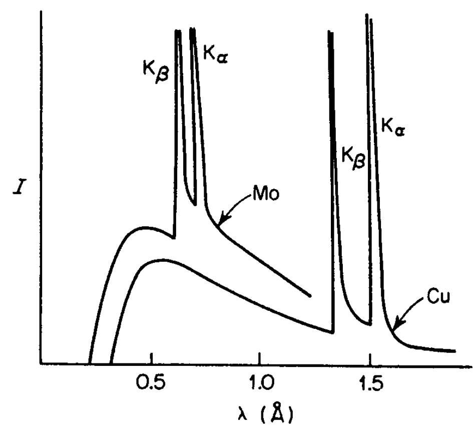

Figure 2.2 X-ray Spectra with characteristic peaks: Mo $K\alpha$ at 50 kV;
Cu $K\alpha$ at 35 kV (Stout & Jensen, 1968)

The distribution of intensity is primarily dependent on the accelerating voltage and only to a smaller extent of the target material. In addition, X-ray spectra show a number of sharp peaks of high intensity whose positions change from one material to another (Figure 2.2). These peaks are characteristic lines for the element of the target material. When the electrons bombarding the target reach the threshold potentials, they are capable of knocking electrons out of their innermost atomic orbitals. At a certain energy value, they can remove electrons from the innermost shell (*K* shell). This causes a vacancy in the *K* shell and it is filled by the descent of an electron from the higher shells (*L* or *M* shells). The difference in potential energy from the higher to the lower level appears as radiation. A nearly monochromatic transition line is given out as the energy levels of the shells are well defined. The principal peaks are given as

$K_{\alpha 1}, K_{\alpha 2}$ $\quad L \rightarrow K$

$K_{\beta 1}, K_{\beta 2}$ $\quad M \rightarrow K$

The characteristic lines shift to shorter wavelength as the atomic number, *Z* of the target material increases. In principle, almost any desired value for the K_{α} line can be obtained by selecting an appropriate target material.

For X-ray diffraction analysis, the radiation used should be as nearly monochromatic as possible. The K_{α} lines fulfill this requirement, but the presence of the accompanying K_{β} lines is a nuisance. To overcome this, crystal monochromator can be used to remove the K_{β} line (Stout & Jensen, 1968).

2.1.1 X-ray Tube

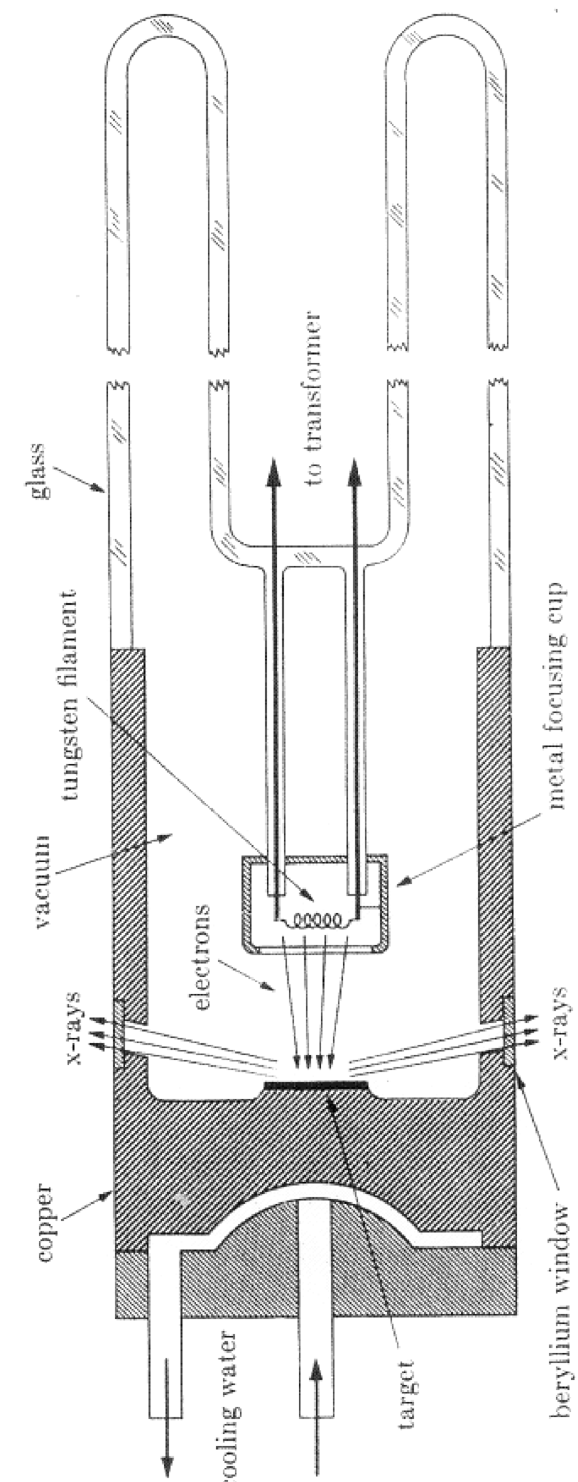

Figure 2.3 Cross-sectional schematic of a sealed filament X-ray tube (Cullity, 1967)

The internal construction of a sealed filament X-ray tube is shown in Figure 2.3. It consists of an evacuated glass envelope which insulates the anode at one end from the cathode at the other end. One lead of the high-voltage transformer (normally 30 to 50 kV for X-ray diffraction work) is connected to the filament and the other is grounded. The target anode is being grounded by its own water cooling system. Electrons emitted by the heated tungsten filament being rapidly accelerated to the target anode by the high voltage across the tube. The focusing cup, which is a small metal cup surrounding the heated filament, repels the electrons and focuses them into a narrow region of the target, so-called the focal spot. X-ray radiations are emitted from the focal spot in all directions and leave the tube through two or more windows which are normally made of beryllium.

The conversion of incident energy of the electron beam into X-rays is a very inefficient process. Less than 1 % of incident energy is converted into X-ray radiations, the remaining heat energy is dissipated by the water cooling system. The most important properties of deciding an X-ray tube is the choice of the target material and the radiation filter. For single crystal diffraction work, Mo and Cu tubes are adequate for 99 % of all problems. The size and shape of the focal spot and the power are important as well since the X-ray intensity depends on these two parameters. Within limits, the size of the focal spot should be as small as possible in order to concentrate the electron energy into a small area of the target and hence produce a high-intensity beam of X-rays. The maximum power rating is the limit of amount of heat that can be dissipated by the target without damage to the X-ray tube (Cullity, 1967).

2.2 Crystal Systems

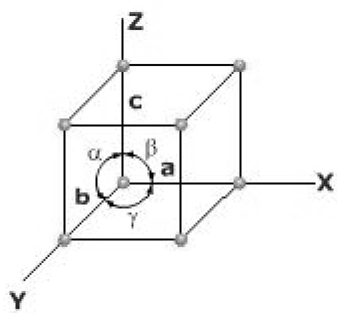

Figure 2.4 Unit Cell

There are seven three-dimensional coordinate systems which are useful in describing crystals and they are the basis for the classification. Generally, a unit cell is characterized by six parameters, *i.e.* the three axial lengths (a, b and c) and three inter-axial angles (α, β and γ) (Figure 2.4). By giving special values to these parameters, we can produce unit cells of various shapes and therefore various types of point lattices. It turns out that only seven different types of cells are necessary to include all the possible point lattices. These correspond to the seven crystal systems into which all crystals can be classified and they are listed in Table 2.1.

Table 2.1 The seven crystal systems (Stout & Jensen, 1967)

Crystal system	No. of independent Parameters	Parameters	Lattice symmetry
Triclinic	6	$a \neq b \neq c$; $\alpha \neq \beta \neq \gamma$	$\bar{1}$
Monoclinic	4	$a \neq b \neq c$; $\alpha = \gamma = 90°; \beta \neq 90°$	$\frac{2}{m}$
Orthorhombic	3	$a \neq b \neq c$; $\alpha = \beta = \gamma = 90°$	mmm
Tetragonal	2	$a = b \neq c$; $\alpha = \beta = \gamma = 90°$	$\frac{4}{m}mm$
Rhombohedral	2	$a = b = c$; $\alpha = \beta = \gamma \neq 90°$	$\bar{3}m$
Hexagonal	2	$a = b \neq c$; $\alpha = \beta = 90°; \gamma = 120°$	$\frac{6}{m}mm$
Cubic	1	$a = b = c$; $\alpha = \beta = \gamma = 90°$	$m3m$

Different primitive point lattices can simply be obtained by putting points at the corners of the unit cell of the seven crystal systems. However, there are other arrangements of points (non-primitive lattices) which fulfill the requirements of a point lattice, namely, that each point has identical surroundings. In 1848, Bravais demonstrated that there are a total of 14 possible point lattices and no more and thus they are called as the Bravais lattices. These 14 Bravais lattices consist of seven primitive and seven non-primitive lattices and they are listed in Table 2.2 (Cullity, 1967).

Table 2.2 The 14 Bravais lattices (Cullity, 1967)

Crystal system	Bravais lattices			
Triclinic	Primitive 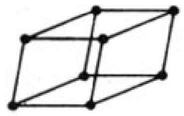			
Monoclinic	Primitive 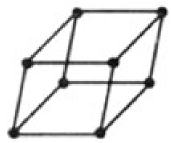	End-centered 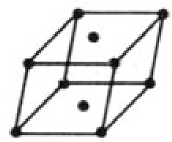		
Orthorhombic	Primitive 	End-centered 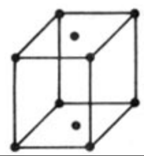	Body-centered 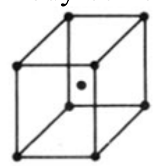	Face-centered 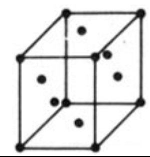
Tetragonal	Primitive 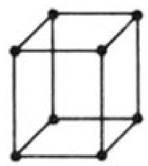	Body-centered 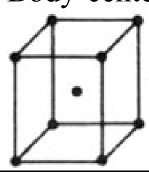		
Rhombohedral	Primitive 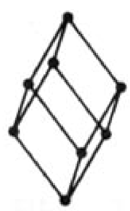			
Hexagonal	Primitive 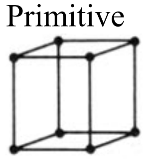			
Simple cubic	Primitive 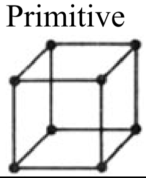	Body-centered 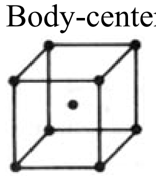	Face-centered 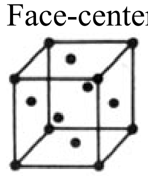	

2.3 X-ray Diffraction

Although X-rays had been discovered by Roentgen in 1895, but their nature was not known. Following the experimental observation of X-ray diffraction in early 1912, Max von Laue showed that the wave characteristics of X-ray could be described in terms of diffraction from a three-dimensional grating. In the same year, W. L. Bragg noticed the similarity of diffraction to ordinary reflection and therefore he deduced a simple equation treating diffraction as “reflection” from planes in the lattice, deriving the well-known Bragg’s Law.

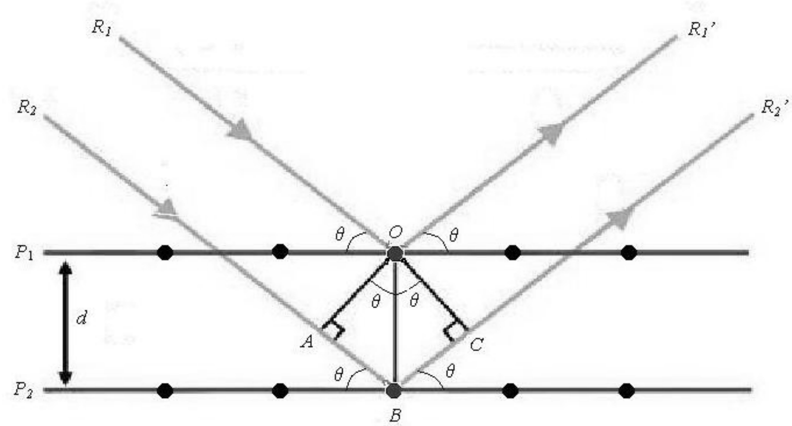

Figure 2.5 Construction showing conditions for diffraction

Consider an X-ray beam incidents on two parallel planes (P_1 and P_2) with inter-planar spacing of *d* (Figure 2.5). The parallel incident rays (R_1 and R_2) make an angle of θ with these incident planes. Assume that electrons at *O* and *B* will be forced to vibrate by the oscillating field of the incident beam and they will radiate in all directions as vibrating charges. For that particular direction where the parallel secondary rays (R_1' and R_2') emerge at angle θ as it reflected from the planes, a diffracted beam of maximum intensity will result if the waves represented by these rays are in phase. It can be shown that $\angle AOB = \angle BOC = \theta$ by dropping perpendicular from O to A and O to C, respectively. Therefore, $AB = BC$, and waves in ray R_2' will be in phase with those in R_1' if $AB + BC$ is an integral number of wavelengths λ ($AB + BC = 2AB$). This can be expressed by the equation

$$2AB = n\lambda \tag{2.3}$$

where n is an integer.

Using $\frac{AB}{OB} = \frac{AB}{d} = \sin\theta$, (2.3) becomes

$$2d\sin\theta = n\lambda \tag{2.4}$$

(2.4) is the Bragg's Law.

Since $\sin\theta \leq 1$

$$\frac{n\lambda}{2d} \leq 1 \tag{2.5}$$

When $n = 1$

$$\lambda \leq 2d \tag{2.6}$$

From (2.6), we notice that the radiation used must have wavelengths comparable to or smaller than twice the inter-atomic spacing, d in the crystal structure (Stout & Jensen, 1968).

2.3.1 Reciprocal Lattice

Consider Bragg's Law (2.4) in the form of

$$\sin\theta = \frac{n\lambda}{2d} \tag{2.7}$$

It can be seen than $\sin\theta$ is inversely proportional to the inter-planar spacing in the crystal lattice. Since $\sin\theta$ is a measure of the deviation of the diffracted beam from the direct beam, it is evident that crystal structures with large *d* will exhibit compressed diffraction patterns, and conversely for small *d*. Interpretation of X-ray diffraction patterns would be facilitated if the inverse-relation between $\sin\theta$ and *d* could be replaced by a direct one. This can be achieved by constructing a reciprocal lattice based on $1/d$, a quantity that varies directly as $\sin\theta$ (Stout & Jensen, 1968).

Relationships between direct and reciprocal lattices:

$$a = \frac{b^*c^*\sin\alpha^*}{V^*}; \qquad a^* = \frac{bc\sin\alpha}{V} \tag{2.8}$$

$$b = \frac{c^*a^*\sin\beta^*}{V^*}; \qquad b^* = \frac{ca\sin\beta}{V} \tag{2.9}$$

$$c = \frac{a^*b^*\sin\gamma^*}{V^*}; \qquad c^* = \frac{ab\sin\gamma}{V} \tag{2.10}$$

$$V = abc[1-\cos^2\alpha-\cos^2\beta-\cos^2\gamma+2\cos\alpha\cos\beta\cos\gamma]^{1/2} \tag{2.11}$$

$$V^* = a^*b^*c^*[1-\cos^2\alpha^*-\cos^2\beta^*-\cos^2\gamma^*+2\cos\alpha^*\cos\beta^*\cos\gamma^*]^{1/2} \tag{2.12}$$

2.3.2 Bragg's Law in Reciprocal Space

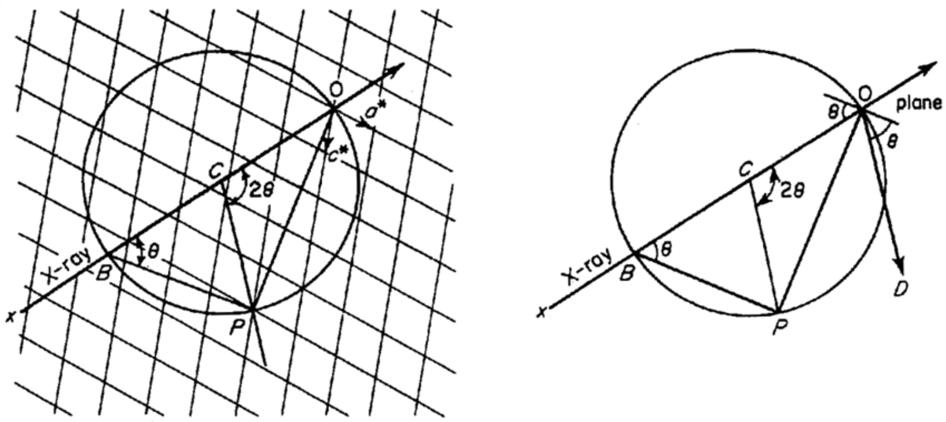

(a) (b)

Figure 2.6 Diffraction in terms of the reciprocal lattice:

(a) The reciprocal lattice and the sphere of reflection

(b) The direct plane (Stout & Jensen, 1968)

Imagine a crystal is placed in an X-ray beam of wavelength, λ. Assume that the crystal is oriented in such a way that the X-ray beam lies on the reciprocal lattice a^*c^* plane (Figure 2.6a). The line *XO* is in the direction of the beam passing through the reciprocal lattice origin *O*. A sphere of radius $1/\lambda$ with its center *C* on *XO* and located so that *O* falls on the circumference of the big circle. Consider the properties of a reciprocal lattice point *P* lying on this circle. The angle *OPB* is inscribed in a semicircle and thus is a right angle. Therefore

$$\sin OBP = \sin\theta = \frac{OP}{OB} = \frac{OP}{2/\lambda} \tag{2.13}$$

$$\sin\theta = \frac{OP}{2}\lambda \tag{2.14}$$

Since *P* is a reciprocal lattice point, the length of *OP* is by definition equal to $1/d_{hkl}$. Substituting $OP = 1/d_{hkl}$

$$\sin\theta = \frac{\lambda}{2d_{hkl}} \tag{2.15}$$

$$2d\sin\theta = \lambda \tag{2.16}$$

(2.16) is just the Bragg's Law with $n = 1$.

Generally, this derivation implies that Bragg's law is fulfilled and reflection occurs whenever a reciprocal lattice point coincides with a circle constructed as described. The reflecting plane is perpendicular to *OP*, hence parallel to *BP* and it makes an angle of θ with *OB*. The direction of reflection is along *OP*. The construction is not limited to the a^*c^* section but holds for the whole sphere, the sphere of reflection. Thus for any point lying on the surface of this sphere, the same conditions hold as for point *P* in Figure 2.6 and the conditions for Bragg's Law reflection are fulfilled for the related direct space plane. By rotating the lattice about its origin, various reciprocal lattice points can be brought into coincidence with the surface of sphere of reflection and the corresponding reflection can be observed.

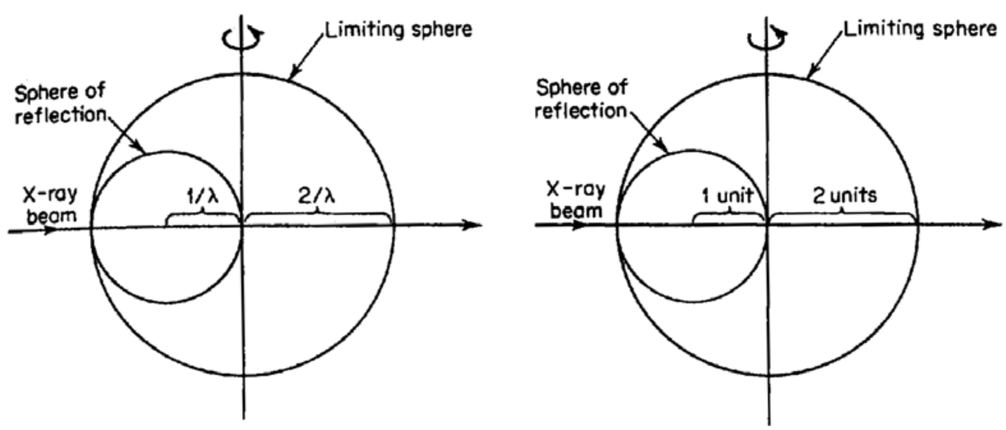

Figure 2.7 Sections through the sphere of reflection and the limiting sphere:
(a) for reciprocal lattice defined as $1/d$
(b) for reciprocal lattice defined as λ/d (Stout & Jensen, 1968)